Int. J. Solids Structures Vol. 16, pp. 1037–1049
© Pergamon Press Ltd., 1980. Printed in Great Britain

0020-7683/80/1101-1037/$02.00/0

DYNAMIC LARGE-DISPLACEMENT ANALYSIS OF CURVED BEAMS INVOLVING SHEAR DEFORMATION

IZHAK SHEINMAN
Faculty of Civil Engineering, Technion—Israel Institute of Technology, Haifa, Israel

(*Received* 17 *March* 1980)

Abstract—A general analytical and numerical procedure, based on large deflection and small rotation, is developed for an arbitrary plane curved beam made of linear elastic material and subjected to arbitrary dynamic loading. The equations of motion admit shear deformation, rotary inertia, geometrical initial imperfections and viscous damping. The numerical solution is obtained by reduction of the nonlinear equations to a linear sequence by a modification of Newton's method, conversion of the differential equations to finite difference equations and application of Houbolt's method in the time domain. Three numerical examples involving dynamic buckling are presented and the influence of shear stiffness is considered.

NOTATION

A area
$[\tilde{A}]$ overall stiffness matrix
b width of beam
$[\tilde{C}]$ overall damping matrix
C^{ijkl} tensor of elastic coefficients
e_i base vector
E modulus of elasticity
EVW external virtual work
$G_{\alpha\beta}$ metric tensor
G determinant of $G_{\alpha\beta}$
G shear modulus
GA_s shear stiffness
h depth of beam
IVW internal virtual work
m external moment
M bending moment
N unit normal vector
N axial force
p_S, p_N external load in ζ^1- and ζ^2-directions
Q shear force
r position vector to axis
R position vector of any point in plane of beam
R radius
$[R]$ mass matrix
S^{ij} Kirchhoff stress tensor
t time
T unit tangent vector
u_α component of displacement
u tangent displacement (unknown)
$\bar{u}$ tangent geometric imperfection
v displacement vector
V volume
w normal displacement (unknown)
$\bar{w}$ normal geometric imperfection
$\{z\}$ unknown vector
ϕ rotation (unknown)
ρ mass density
χ curvature
σ^{ij} stress tensor
ω_i angle frequency
ϵ_{ij} strain tensor
ζ^1, ζ^2 coordinates
ζ_i damping ratio
$[\alpha, \beta, \gamma]$ Christoffel symbol of first kind
$\Gamma^\gamma_{\alpha\beta}$ Christoffel symbol of second kind
$(\,)'$ $d/d_\zeta{}^1(\,)$
$(\dot{})$ $d/d_t(\,)$
$(\,)_{,}$ covariant differentiation
$(\tilde{})$ referred to deformed beam

1. INTRODUCTION

Although large deflection of arches has been the subject of numerous investigations (see, e.g. Refs. [1–7]) only a few of them admit shear deformation. The first attempt to derive the static nonlinear equations for a beam with shear deformation was made in Ref. [5]; more exact analyses for beams and arches are reported in Ref. [6]. A nonlinear dynamic theory of thin straight beams with shear deformation and rotary inertia is derived in Ref. [7]. None of these cover an arbitrary curved beam,—and furthermore they are more concerned with deviations and with qualitative aspects, than with the solution procedure and the quantitative effect of shear deformation.

In the present work, which extends the analysis in Ref. [8] to the case of large deflection and small rotation, a general dynamic theory and a solution procedure are developed for an arbitrary curved beam made of linear elastic material with geometrical initial imperfections. Shear deformation, rotary inertia and viscous damping are taken into account and the quantitative influence of the shear stiffness is examined. Shear deformation and rotary inertia, with their effect on nonlinear characteristics, come into play in such problems as thick and layered structures and higher-mode vibration.

The nonlinear equations of motion for a plane curved beam of arbitrary shape, written in tensor form, are derived from the general three-dimensional theory. The kinematic variables, the parameters of the geometrical initial imperfection and the equations of motion are referred to the initial configuration (generally being called "Lagrangian formulation"). By recourse to the shear-angle parameter, the Kirchhoff hypothesis is replaced with a Bernoulli-type one (that normals to the pre-deformation reference surface do not necessarily retain their normality after deformation). The kinematic unknowns are chosen so as to yield a second-order nonlinear differential equation. Finally, the proposed numerical solution procedure consists in reduction of the nonlinear differential equations to a linear sequence by means of a modification of Newton's method [9], conversion of the differential equations to finite-difference equations with interlaced nets [8, 10] and application of Houbolt's method [11] in the time domain.

The theory and solution procedure are illustrated on the examples of a straight beam, a shallow arch and a deep arch. In all three, subjected to a step load, the dynamic buckling behavior was studied and the influence of shear deformation was examined.

2. ANALYTICAL FORMULATION

The governing differential equations and the appropriate boundary conditions are derived for an arbitrary curved beam under dynamic loading. The equations include the effect of shear deformation and rotary inertia.

Some parts of the procedure are as in Ref. [8], but are recapitulated here for the sake of completeness. All kinematic and load variables are functions of the time parameter (t), but the index t is omitted for convenience.

Geometry

In a plane beam, all material properties as well as the external loading are symmetric with respect to a plane containing the axis of the beam. Let x, y (Fig. 1) be the plane of symmetry, and let the pre-deformation axis be described by the position vector $\mathbf{r}(\zeta^1)$ (ζ^1 denoting the axial length). The following geometrical relations hold at every point of the axis:

$$\mathbf{T} = \frac{d\mathbf{r}}{d_{\zeta^1}}; \quad \frac{d\mathbf{T}}{d_{\zeta^1}} = -\chi\mathbf{N}; \quad \frac{d\mathbf{N}}{d_{\zeta^1}} = \chi\mathbf{T} \tag{1}$$

where T is the unit tangent vector. N is the unit normal vector and χ is the beam curvature.

The position vector of any point in the plane can be given by:

$$\mathbf{R}(\zeta^1, \zeta^2) = \mathbf{r}(\zeta^1) + \zeta^2\mathbf{N}(\zeta^1) \tag{2}$$

where ζ^2 denotes length along the normal. The coordinates ζ^1, ζ^2 are seen to be "natural" for

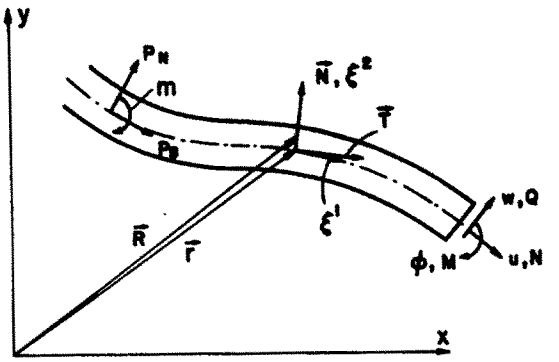

Fig. 1. Coordinates, displacements, external and internal forces.

analysis of a curved beam. The base vectors of the system are

$$\mathbf{e}_1 = (1 + \zeta^2\chi)\mathbf{T}$$
$$\mathbf{e}_2 = \mathbf{N}. \tag{3}$$

The metric tensor defined as $G_{ij} = \mathbf{e}_i\mathbf{e}_j$ has the following equalities for its components:

$$G_{11} = (1 + \zeta^2\chi)^2; \qquad G^{11} = 1/G_{11}$$
$$G_{12} = G_{21} = 0; \qquad G_{22} = G^{22} = 1. \tag{4}$$

The Christoffel symbols of the first and second kind are:

$$[\alpha, \beta, \gamma] = 1/2\left[\frac{\partial G_{\alpha\gamma}}{\partial\zeta^\beta} + \frac{\partial G_{\beta\gamma}}{\partial\zeta^\alpha} - \frac{\partial G_{\alpha\beta}}{\partial\zeta^\gamma}\right]$$
$$\Gamma^\gamma_{\alpha\beta} = G^{\gamma\rho}[\alpha\beta, \rho]. \tag{5}$$

Substitution of eqn (4) in (5) yields:

$$[11, 1] = (1 + \zeta^2\chi)\chi'\zeta^2 \quad \Gamma^1_{11} = \chi'\zeta^2/(1 + \xi^2\chi)$$
$$[11, 2] = -\chi(1 + \zeta^2\chi) \quad \Gamma^2_{11} = -\chi/(1 + \zeta^2\chi)$$
$$[12, 1] = \chi(1 + \xi^2\chi) \quad \Gamma^1_{12} = \chi/(1 + \zeta^2\chi)$$
$$[21, 1] = \chi(1 + \zeta^2\chi) \quad \Gamma^1_{21} = \chi/(1 + \zeta^2\chi). \tag{6}$$

Kinematics

The basic assumptions of the beam theory used here are that plane sections normal to the beam axis before deformation retain their planeness but not necessarily their normality after deformation, and that normal strain is neglected. The deformation can be described in terms of a pair of vector functions with ζ^1 as the only variable:

$$\mathbf{v}(\zeta^1, \zeta^1) = \mathbf{v}_1(\zeta^1) + \zeta^2\mathbf{v}_2(\zeta^1) \tag{7}$$

and the post-deformation position vector is given by

$$\tilde{\mathbf{R}}(\zeta^1, \zeta^2) = \mathbf{r}(\zeta^1) + \mathbf{v}_1(\zeta^1) + \zeta^2(\mathbf{N}(\zeta^1) + \mathbf{v}_2(\xi^1)). \tag{8}$$

The displacement vectors can be expressed in terms of their components in the initial configurations as follows:

$$\mathbf{v}_1(\zeta^1) = u\mathbf{T} + w\mathbf{N}$$
$$\mathbf{v}_2(\zeta^1) = \phi\mathbf{T}. \tag{9}$$

where u and w are the displacements of the natural surface in the ζ^1- and ζ^2-directions, respectively; ϕ is its angular rotation (all three being scalar functions of ζ^1).

Substitution of eqn (9) in (7) yields:

$$\mathbf{v}(\zeta^1, \zeta^2) = (u + \zeta^2\phi)\mathbf{T} + w\mathbf{N}. \tag{10}$$

The projections of the displacement on the base vectors read:

$$\begin{aligned} &u_\alpha = \mathbf{v}\mathbf{e}_\alpha \\ &u_1 = (1 + \zeta^2\chi)(u + \zeta^2\phi);\ u^1 = (u + \zeta^2\phi)/(1 + \zeta^2\chi) \\ &u_2 = w;\ u^2 = w. \end{aligned} \tag{11}$$

The strain tensor is given by:

$$\epsilon_{\alpha\beta} = 1/2(\tilde{G}_{\alpha\beta} - G_{\alpha\beta}) = 1/2(u_{\alpha,\beta} + u_{\beta,\alpha} + G_{\gamma\delta}u^\gamma{}_{,\alpha} \cdot u^\delta{}_{,\beta}). \tag{12}$$

In the case of a geometrical initial imperfection, we visualize initial displacements $\bar{u}$, $\bar{w}$ (in the tangential and normal directions, respectively) and initial rotation $\bar{\phi}$, in the unloaded (stress-free) beam and redefine the strain tensor:

$$\epsilon_{\alpha\beta} = \epsilon_{\alpha\beta}(u + \bar{u}, w + \bar{w}, \phi + \bar{\phi}) - \epsilon_{\alpha\beta}(\bar{u}, \bar{w}, \bar{\phi}) \tag{13}$$

and its components are obtained by covariant differentiation, bearing in mind eqns (6), (11). For moderately small rotation, we set $\bar{\phi} = 0$ and with the nonlinear terms of ϕ and ϕ' neglected, the strain components are:

$$\begin{aligned} \epsilon_{11} &= u' + \chi w + \chi^2/2u^2 + \chi^2/2w^2 + 1/2u'^2 + 1/2w'^2 + \chi u'w - \chi w'u \\ &\quad + u'\bar{u}' + w'\bar{w}' + \chi^2 u\bar{u} + \chi^2 w\bar{w} + \chi u'\bar{w} + \chi\bar{u}'w - \chi w'\bar{u} - \chi\bar{w}'u \\ &\quad + \zeta^2(\phi' + \chi u' + \chi^2 w) + (\xi^2)^2\chi\phi' \\ \epsilon_{12} &= 1/2(\phi + w' - \chi u) \\ \epsilon_{22} &= 0. \end{aligned} \tag{14}$$

(Note that in the theory which disregards shear deformation, ϕ is no longer independent of u and w.)

Equations of motion

The equations of motion are derived by the principle of virtual displacements, which postulates equality of the internal and external virtual work:

$$\mathrm{IVW} = \mathrm{EVW}. \tag{15}$$

The internal virtual work is given by:

$$\mathrm{IVW} = \int_{\tilde{V}} \tilde{\sigma}^{ij}\delta\tilde{\epsilon}_{ij}\,\mathrm{d}\tilde{V} \tag{16}$$

where $\tilde{\sigma}^{ij}$ and $\tilde{\epsilon}_{ij}$ are the stress- and strain tensors referred to the deformed system and $\tilde{V}$ is the post-deformation value. Resorting to the Kirchhoff stress tensor in the underformed system:

$$S^{ij} = \frac{\mathrm{d}\tilde{V}}{V}\tilde{\sigma}^{ij} = \sqrt{\left(\frac{\tilde{G}}{G}\right)}\tilde{\sigma}^{ij}. \tag{17}$$

(G and $\tilde{G}$ being, respectively, the pre- and post-deformation determinant of the metric tensor),

the internal virtual work can likewise be expressed (see Ref. [12]) as:

$$\mathrm{IVW} = \int_V S^{ij}\delta\epsilon_{ij}\,\mathrm{d}V \tag{18}$$

and assuming that the stress–strain relation is

$$S^{ij} = C^{ijkl}\epsilon_{kl} \tag{19}$$

where C^{ijkl} is the tensor of elastic properties, substitution of eqn (19) in (18) yields:

$$\mathrm{IVW} = \int_V C^{ijkl}\epsilon_{kl}\delta\epsilon_{ij}\,\mathrm{d}V. \tag{20}$$

The external virtual work, incorporating the influence of inertial forces, is

$$\mathrm{EVW} = \int_{\xi^1}(p_s\delta u + p_N\delta w + m\delta\phi)\,\mathrm{d}\xi^1 - \int_V \rho\ddot{\mathbf{v}}\delta\mathbf{v}\,\mathrm{d}V + N^*\delta u^* + Q^*\delta w^* + M^*\delta\phi^* \tag{21}$$

where p_s and p_N are the loads in ξ^1- and ξ^2-directions respectively, m is the external moment (see Fig. 1), ρ is the mass density, N^*, Q^*, $M^*$are the external forces at the boundaries and u^*, w^*, ϕ^* are the corresponding displacements.

Substitution of eqn (10) in (21) yields

$$\mathrm{EVW} = \int_{\xi^1}(p_s\delta u + p_N\delta w + m\delta\phi)\,\mathrm{d}\xi^1 - \int_V \rho\{(\ddot{u} + \xi^2\ddot{\phi})(\delta u + \xi^2\delta\phi) + \ddot{w}\delta w\}\,\mathrm{d}V$$

$$+ N^*\delta u^* + Q^*\delta w^* + M^*\delta\phi^*. \tag{22}$$

(Note that the only type of load considered here is one which preserves its magnitude and orientation under deformation, and is specified accordingly as force per unit underformed length.)

Substituting eqns (14) in (20), integrating the latter by parts and referring to eqn (15), we obtain the equations of motion as a set of second-order nonlinear differential equations in u, w and ϕ, which read in implicit form as follows:

$$\begin{aligned}
&[{}_0M^{11}(1 + u' + \chi w + \bar{u}' + \chi\bar{w})]' - {}_0M^{11}\chi[\chi u - w' + \chi\bar{u} - \bar{w}'] + {}_0M^{12}\chi + p_s = {}_0I\ddot{u} + {}_1I\ddot{\phi}\\
&[{}_0M^{11}(w' - \chi u + \bar{w}' - \chi\bar{u}) + {}_0M^{12}]' - {}_0M^{11}\chi[1 + \chi w + u' + \chi\bar{w} + \bar{u}'] + {}_1M^{11}\chi^2 + p_N = I_0\ddot{w}\\
&[{}_1M^{11} + {}_2M^{11}\chi]' - {}_0M^{12} + m = {}_1I\ddot{u} + {}_2I\ddot{\phi}
\end{aligned} \tag{23}$$

with the following boundary conditions:

$$\begin{aligned}
&u = u^* \text{ or } {}_0M^{11}(1 + u' + \chi w + \bar{u}' + \chi\bar{w}) + {}_1M^{11}\chi = N^*\\
&w = w^* \text{ or } {}_0M^{11}(w' - \chi u + \bar{w}' - \chi\bar{u}) + {}_0M^{12} = Q^*\\
&\phi = \phi^* \text{ or } {}_1M^{11} + {}_2M^{11} = M^*
\end{aligned} \tag{24}$$

where

$$\begin{aligned}
{}_nM^{ij} &= \int_A S^{ij}(\xi^2)^n\,\mathrm{d}A\\
{}_nI &= \int_A \rho(\xi^2)^n\,\mathrm{d}A
\end{aligned} \tag{25}$$

${}_nM^{ij}$ are the generalized forces (for example, ${}_0M^{11}$ is the axial force, M^{11} is the bending moment and ${}_0M^{12}$ is the shear force).

Define

$$C_n^{ijkl} = \int_{\xi^2} C^{ijkl}(\xi^2)^n b \, d\xi^2 \tag{26}$$

where b is the width of the beam.

The reference surface is best chosen so that

$$\left.\begin{aligned} C_n^{ijkl} &= 0 \\ {}_nI &= 0 \end{aligned}\right\} \text{ for } n = 1, 3, 5\ldots \tag{27}$$

Substituting eqn (19) in (25) and using eqns (14) and (27), we obtain the generalized forces as function of the displacements:

$$\begin{aligned} {}_0M^{11} &= C_0{}^{1111}e + C_2{}^{1111}\chi\phi' + C_0{}^{1112}\gamma \\ {}_1M^{11} &= C_2{}^{1111}K \\ {}_2M^{11} &= C_2{}^{1111}e + C_4{}^{1111}\chi\phi' + C_2{}^{1112}\gamma \\ {}_0M^{12} &= C_0{}^{1211}e + C_2{}^{1211}\chi\phi' + C_0{}^{1212}\gamma \end{aligned} \tag{28}$$

where

$$\begin{aligned} e &= u' + \chi w + \chi^2/2u^2 + \chi^2/2w^2 + 1/2u'^2 + 1/2w'^2 + \chi u'w - \chi w'u \\ &\quad + u'\bar{u}' + w'\bar{w}' + \chi^2 u\bar{u} + \chi^2 w\bar{w} + \chi u'\bar{w} + \chi\bar{u}'w - \chi w'/\bar{u} - \chi\bar{w}'u \\ K &= \phi' + \chi u' + \chi^2 w \\ \gamma &= \phi + w' - \chi u \end{aligned} \tag{29}$$

(which are generally called extensional, bending and shear strain respectively).

3. SOLUTION PROCEDURE

A modification of Newton's method (Ref. [9]), applicable to differential equations, is employed for reducing the nonlinear field equations eqns (23) and the appropriate boundary conditions eqns (24) to a sequence of linear systems. In this method, the iteration equations are derived by assuming that the solution is achieved by a small correction to an approximate solution (initially taken as the linear solution). These small corrections are obtained through solution of the linearized differential equations.

On substitution of eqns (27)–(29) in (23) and (24) and application of the modified Newton method, the linearized second-order differential equations can be written in matrix form as follows:

Field equations

$$[F_1]\{z''\} + [F_2]\{z'\} + [F_3]\{z\} = \{g_f\} + [R]\{\ddot{z}\}. \tag{30}$$

Boundary equations

$$[B_1]\{z'\} + [B_2]\{z\} = \{g_b\}$$

where $\{z\}^T = \{u, w, \phi\}$ is the unknown vector, $[R]$ is the mass matrix (order 3×3), $[F_i]$ and $[B_i]$ are coefficient matrices (order 3×3) dependent on the geometric and elastic parameters of the beam and on the deformed configuration. $\{g_f\}$ and $\{g_b\}$ are vectors (of order 3) containing the external applied load and terms introduced by the procedure of Newton's method.

These differential equations are recast in the form of finite-difference equations. In view of

the aspects of convergence and accuracy under inclusion of shear deformation, a special finite-difference scheme was chosen, comprising two interlaced distinct nets, one for w and the other for u and ϕ. The first and last equations of eqns (23) are written between mesh points and the second at the points, this yielding a high degree of accuracy even with relatively sparse nets (see Refs. [8, 10]). Differentiation at the boundaries is effected with the aid of fictitious points on either exterior side of the curved beam.

After converting the differential equations to difference equations in the axial direction and adding a viscous damping matrix, the final equations can be written as:

$$[\bar{A}]\{\bar{z}\}+[\bar{C}]\{\dot{\bar{z}}\}+[\bar{R}]\{\ddot{\bar{z}}\}=\{\bar{p}\} \tag{31}$$

where $\{\bar{z}\}^T=\{z_0, z_1 \ldots z_{Np}, z_{Np+1}\}$ is the entire unknown vector (Np is the number of mesh points). $\bar{A}$, $\bar{C}$ and $\bar{R}$ are the overall matrices of stiffness, damping and mass, respectively (all are of order $3(Np+2)\times 3(Np+2)$ and are band matrices).

The exact form of the damping matrix is unknown for most structures, and there is little experimental basis for selecting damping constants. Accordingly, a form of viscous damping proportional to the mass and stiffness matrices, which suffices for most structures, was chosen (see Ref. [13]),

$$[\bar{C}]=\alpha[\bar{R}]+\beta[\bar{A}] \tag{32}$$

α and β are constants, determined from two given damping ratios corresponding to two unequal angular frequencies of vibration:

$$\alpha+\beta\omega_i^2=2\omega_i\xi_i \tag{33}$$

where ω_i are the frequencies and ξ_i the given damping ratios.

The first and second time derivatives of $\bar{z}$ in eqn (31) are approximated by Houbolt's third-order backwards difference expression (see Refs. [8, 11, 13]). The solution for each time step (which later serves as initial solution for the next one) is obtained by an iterative procedure, in which for each iteration the set of equations is solved by the generalization of Potter's method (reported in Ref. [14]), the matrix $\bar{A}$ and vector $\bar{p}$ of eqn (31) being changed accordingly until the solution converges. A time history of the beam response is obtained by using equal increments, either until a prescribed maximum number of time steps has been reached, or until the solution fails to converge after a specified number of iterations. The time interval is usually small, so only a few iterations are required. However, when the curved beam becomes dynamically unstable, the solution may not converge even with a large number of iterations.

4. NUMERICAL RESULTS

A general computer program (DLDCBM) was written for the procedure outlined above, valid for any curved beam under arbitrary dynamic-loading and boundary conditions, as well as for any geometrical initial imperfection. Three examples (worked out on a high-speed IBM 370/168 digital computer) were used for illustrating the above methodology, with the common aim of comparing dynamic and static buckling under step loading at two levels of shear stiffness: (a) a straight beam, (b) a shallow circular arch and (c) a deep circular arch. The static solutions of these examples were obtained by the same program and the results (for a high level of shear stiffness, to which they are also referred in literature) are in very good agreement with Refs. [1, 4] for the shallow arch and with Refs. [2, 3] for the deep arch.

(a) *Straight beam (sine-wave imperfection)*

The parameters and load-frequency curves for this example are given in Fig. 2, as the axial load increases the frequency decreases to a minimum and subsequently increases again. In Ref. [15], the dynamic buckling load was defined as the highest load level for which a bounded response exists, but since the straight beam is stable even beyond the buckling load, a new definition is called for, namely, the load level for which the frequency is minimum. In the

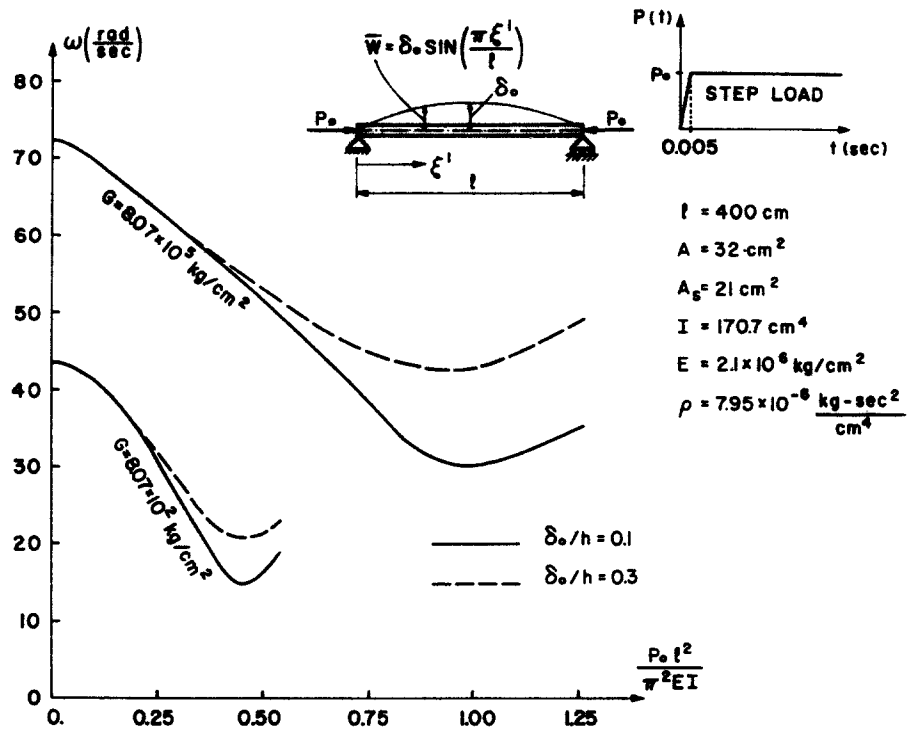

Fig. 2. Load-frequency curves for straight beam under axial step load.

present example the dynamic and static buckling load coincide, as the straight beam is not sensitive to imperfections.

As could be expected, the frequencies and buckling load for the lower level of shear stiffness are lower than for the higher level (see Fig. 2), and while the frequency increases with the imperfection (the beam becoming stiffer because of arching), the buckling load remains the same. The dynamic magnification factor, plotted against the load parameter in Fig. 3, is seen to decrease in the neighborhood of the buckling load. A uniform finite-difference net was chosen with 31 points and the time interval was taken as 1/80 of the period of the first natural mode.

(b) *Shallow circular arch*

The parameters (drawn from Ref. [4]) and load-frequency curves are given in Fig. 4. Here again, as in the preceding example, the frequency decreases to a minimum and then increases. In Fig. 5 the maximum response is plotted for the cases of no damping and critical damping,

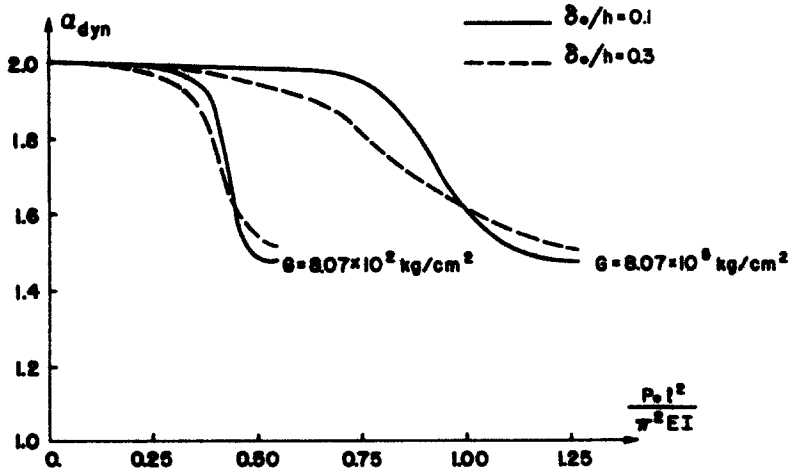

Fig. 3. Dynamic magnification factor for straight beam under axial step load.

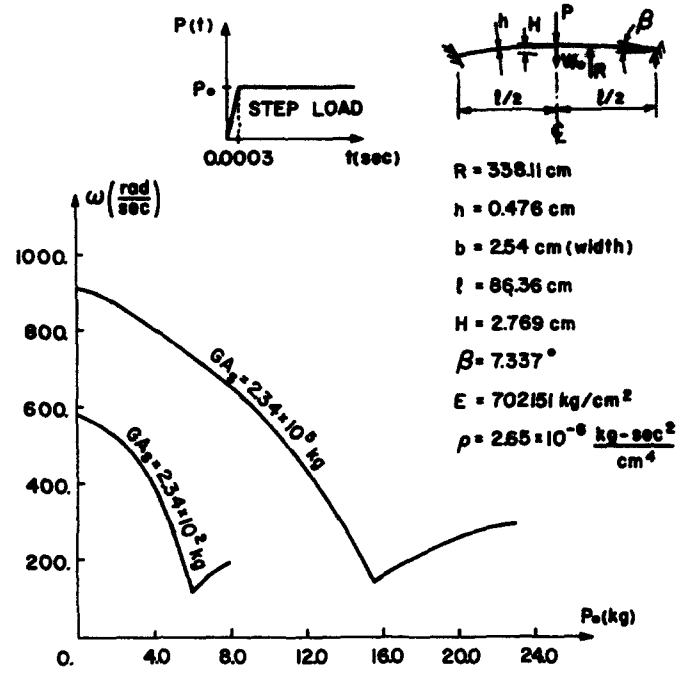

Fig. 4. Load-frequency curves for shallow circular arch under concentrated step load.

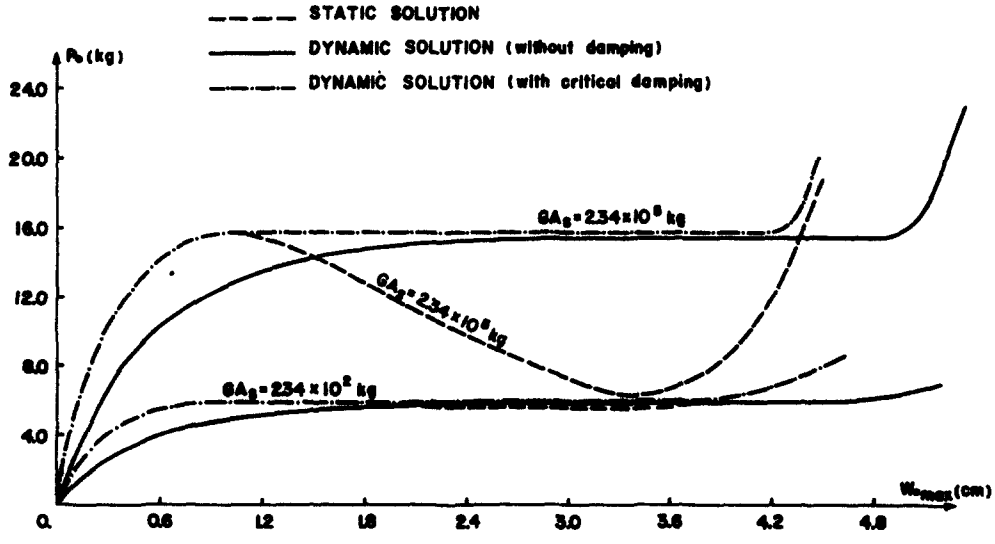

Fig. 5. Maximum static and dynamic apex displacement for shallow circular arch under concentrated step load.

compared with the static solution. In the critical damping case it is the same as in the static solution until a limit point (the minimum point in Fig. 4). When the snap-through occurs the displacement jumps to the other side and stabilizes. Figures 6 and 7 show the time history of the apex displacement at several load levels, plotted for the high and low level of shear stiffness, respectively; since these figures refer to an undamped system, they are compatible with Fig. 4. Houbolt's method contains some built-in damping which depends on the load level and for levels above the limit point a smaller time interval is necessary for an accurate solution. Accordingly the solution is plotted in the above figures for some time intervals in order to illustrate this point. Figure 8, which presents the corresponding time history at critical damping, shows a sharp jump of the response for a small change in load near the limit point (*cf.* $p_0 = 15.2$ and 16 for $GA_s = 2.34 \times 10^5$, $p_0 = 5.0$ and 6.0 for $GA_s = 2.34 \times 10^2$ kg). The jump point is also a characterization of the dynamic buckling load.

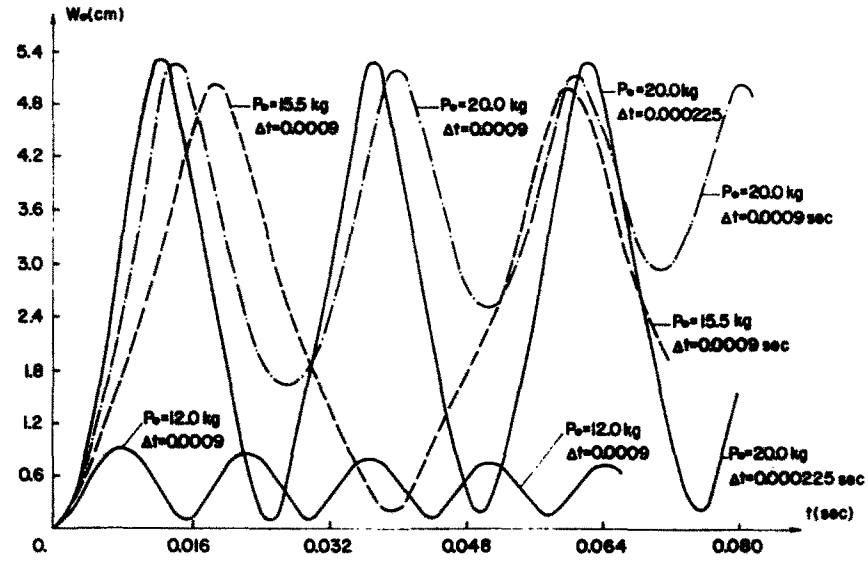

Fig. 6. Time history of apex displacement for shallow arch with $GA_s = 2.34 \times 10^5$ kg.

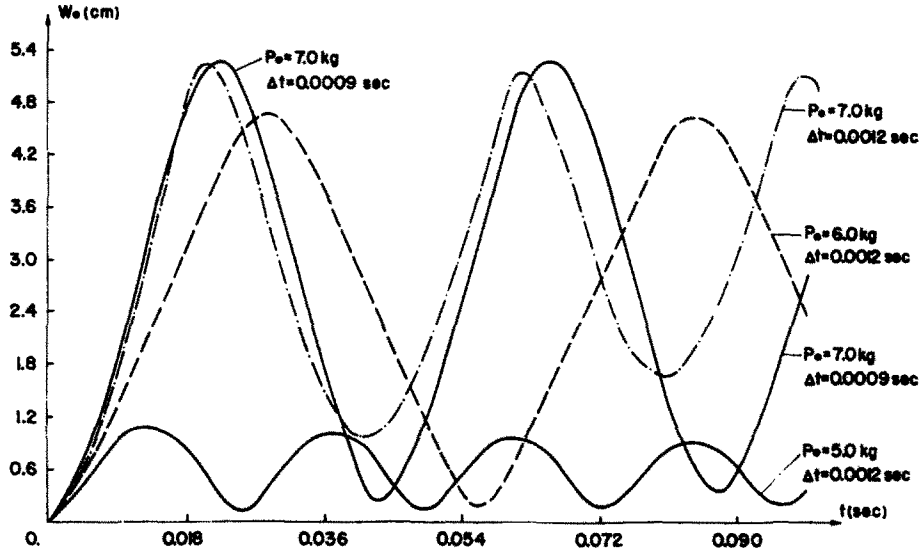

Fig. 7. Time history of apex displacement for shallow arch with $GA_s = 234$ kg.

The dynamic solution converged, with respect to the number of nodal points, by 81 points for the higher stiffness level and by 41 for the lower one. The time interval was taken as 1/100 of the period of the first natural mode.

(c) *Deep circular arch*

The parameters and load-frequency curves are given in Fig. 9; unlike the preceding example, the frequency decreases until there is no bounded response, and the solution failed to converge at the terminal point of these curves (the limit load level). Figure 10 shows the maximum response of the apex displacement for the two stiffness levels and Fig. 11—the time history at some load levels, for the lower stiffness level.

As the anlaysis was confined to the symmetric mode, only one half of the arch was run, subject to the appropriate symmetry condition. The solution for the semicircular arch converged, with respect to the number of nodal points, by 81 points. The time interval was again taken as 1/100 of the period of the first natural mode.

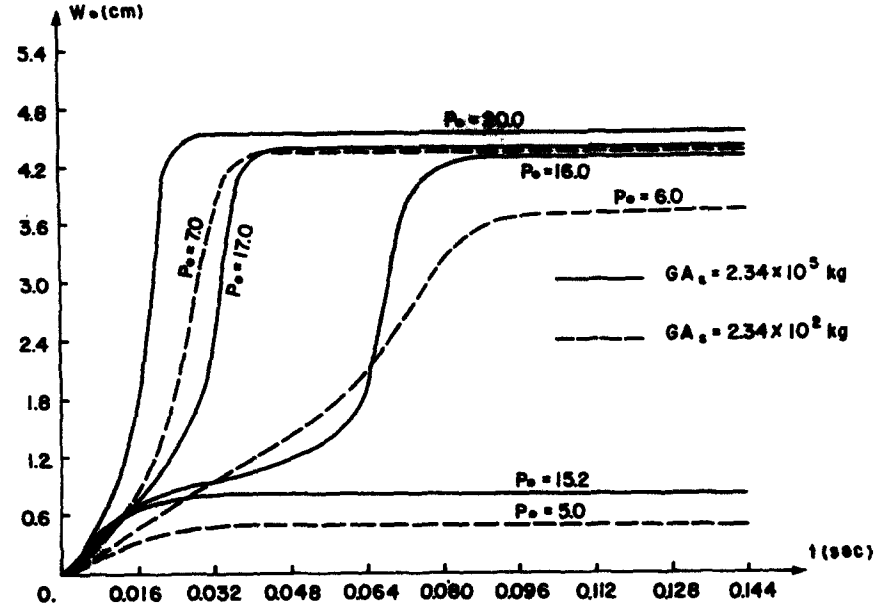

Fig. 8. Time history of apex displacement for shallow arch with critical damping.

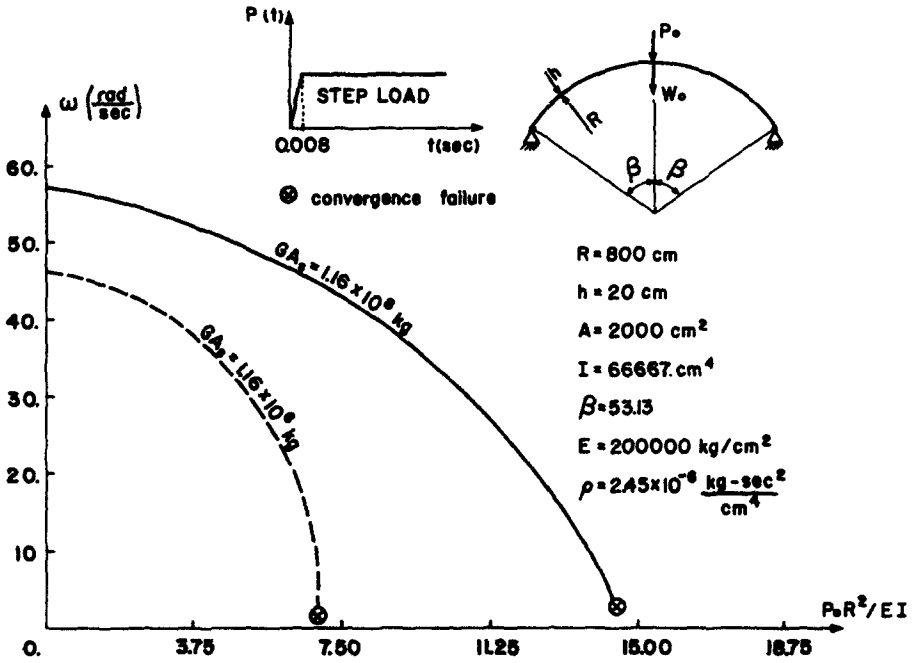

Fig. 9. Load-frequency curves for deep circular arch under concentrated step load.

5. CONCLUSIONS

A non-linear theory, based on large deflection and small rotation and admitting shear deformation and rotary inertia, and a solution procedure, are presented for an arbitrary plane curved beam subjected to arbitrary dynamic loading. The non-linear equations, with the displacements and total rotation as unknowns, are reduced to linear sequences (by a modification of Newton's method), converted to difference equations, and solved by Houbolt's method. The theory (limited to linear elastic material) and the solution procedure are suitable for a wide range of problems, such as layered curved beams with geometric imperfections. The dynamic criteria for buckling, and the influence of shear stiffness, are checked by numerical means.

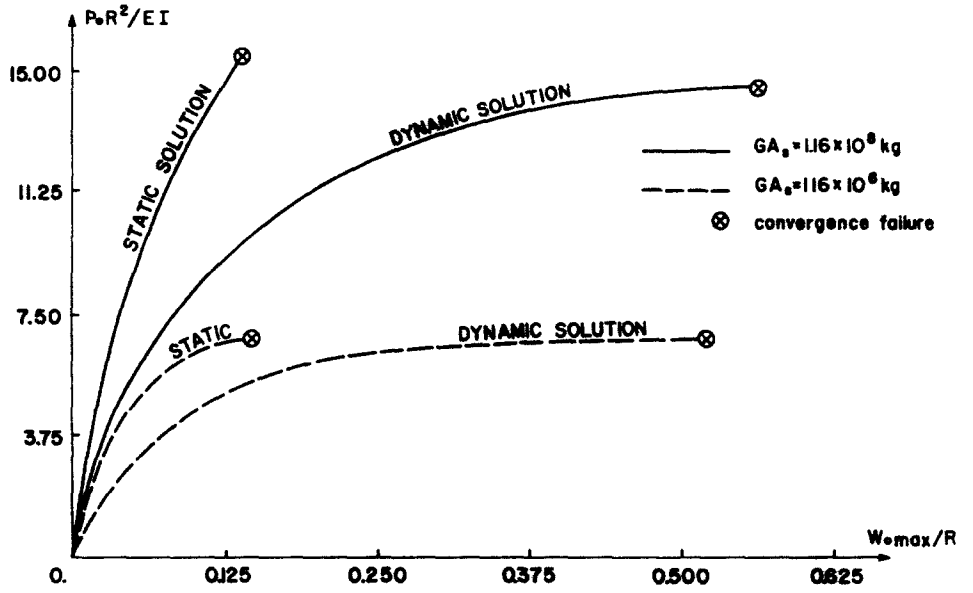

Fig. 10. Maximum static and dynamic displacement for deep circular arch under concentrated step load.

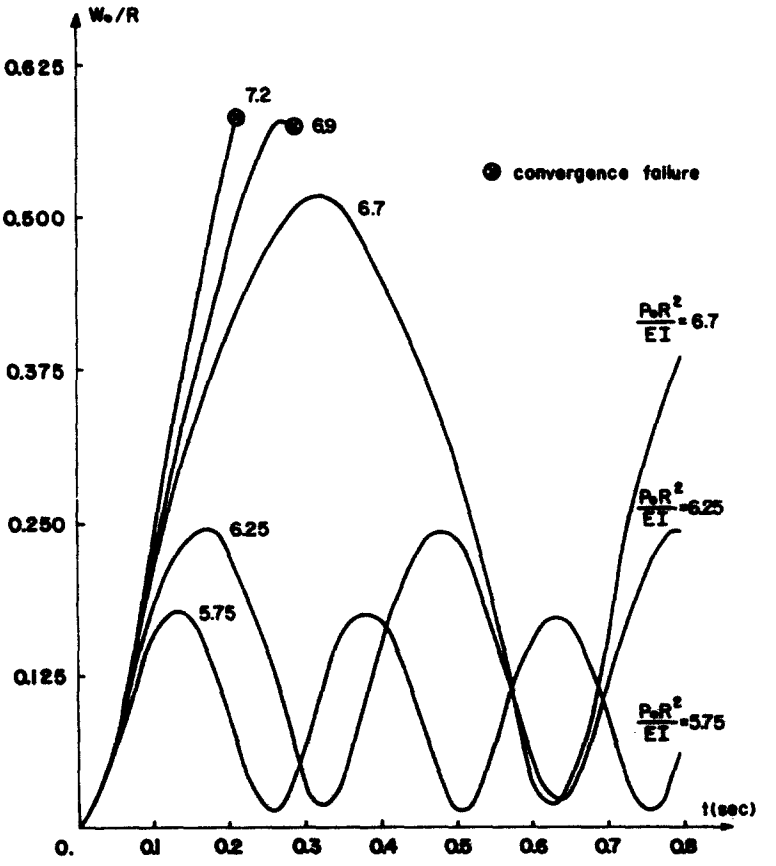

Fig. 11. Time history of apex displacement for deep circular arch with $GA_s = 1.16 \times 10^6$ kg.

REFERENCES

1. A. Gjelsvik and S. R. Bodner, The energy criterion and snap buckling or arches. *J. Engng Mech. Div. Proc. ASCE* **88**, EM5, 87–134 (1962).
2. P. Sharifi and E. Popov, Nonlinear buckling analysis of sandwich arches. *J. Engng Mech. Div. Proc. ASCE* **97**, EM5, 1397–1412 (1971).

3. R. Schmidt and D. A. DaDeppo, Large deflection of eccentrically loaded arches. *Zeitschr. Angew. Math. Phys.* 21(6), 991–1004 (1970).
4. K. Bathe, E. Ramm and E. Wilson, Finite element formulations for large deflection dynamic analysis. *Int. J. Num. Meth. Engng* 9, 353–386 (1975).
5. G. R. Buchanan, D. C. Huang and T. K. M. Cheng, Effect of shear on nonlinear behavior of elastic bars. *J. Appl. Mech., Trans. ASME, Series E* 91(1), 212–215 (1970).
6. D. A. DaDeppo and R. Schmidt, Large deflection of elastic arches and beams with shear deformation. *J. Ind. Math. Soc.* 22(1), 17–33 (1972).
7. S. Y. Lee, On the finite deflection dynamic of thin elastic beams. *J. Appl. Mech.* 38(4), 961–963 (1971).
8. Y. Tene, M. Epstein and I. Sheinman, Dynamics of curved beams involving shear deformation. *Int. J. Solids Structures* 11, 827–840 (1975).
9. G. A. Thurston, Newton's method applied to problems in nonlinear mechanics. *J. Appl. Mech., Trans. ASME Series E* 87, 383–388 (1965).
10. A. K. Noor and V. K. Khasdewal, Improved finite-difference variant for the bending analysis of arbitrary cylindrical shells. *Unicif Rep. No. R-58*, University of New South Wales, Kensington, Australia, (1969).
11. J. G. Houbolt, A recurrence matrix solution for the dynamic response of elastic aircraft. *J. Aeronaut. Sci.* 17, 540 (1950).
12. B. Budiansky, Notes on nonlinear shell theory. *J. Appl. Mech., Trans. ASME* 35, 393–401 (June 1968).
13. I. Sheinman, Forced vibration of a curved beam with viscous damping. *Comp. Structures* 10, 499–503 (1979).
14. Y. Tene, M. Epstein and I. Sheinman, A generalization of Potter's method. *Comp. Structures* 4, 1099–1103 (1974).
15. B. Budiansky, Dynamic buckling of elastic structures: criteria and estimates. In *Dynamic Stability of Structures* (Edited by G. Herrmann). Pergamon Press, Oxford (1966).